AUCTORES
Globalize your Research

Clinical Research and Clinical Trials

Nan Lu *

Open Access

Research Article

Theoretical Investigation on Tf–Dmap/Dmap-Catalyzed Addition–Cyclization of Carboxylic Acid, Crotonate Sulfonium Salt, And Amine to Build 1,2,3-Trisubstituted Pyrrole

Nan Lu

College of Chemistry and Material Science, Shandong Agricultural University, Taian 271018, P. R. China.

***Corresponding Author:** Nan Lu, College of Chemistry and Material Science, Shandong Agricultural University, Taian 271018, P. R. China.

Received date: June 19, 2026; **Accepted date:** July 03, 2026; **Published date:** July 10, 2026

Citation: Nan Lu, (2026), Theoretical Investigation on Tf−Dmap/Dmap-Catalyzed Addition−Cyclization of Carboxylic Acid, Crotonate Sulfonium Salt, And Amine to Build 1,2,3-Trisubstituted Pyrrole, *Clinical Research and Clinical Trials*, 15(5); **DOI:10.31579/2693-4779/329**

Abstract:

The first theoretical investigation on Tf−DMAP/DMAP-catalyzed addition−cyclization of carboxylic acid, crotonate sulfonium and amine was provided by our DFT calculation. First, the deprotonation of allyl sulfonium salt forms its ylide assisted by DMAP. Concurrently, acylpyridinium salt was afforded upon activa-tion of carboxylic acid under the help of TfDMAP giving TfOH. Subsequently, the nucleophilic attack between the above two generates corresponding intermediate, which proceeds double bond shift followed by con-densation of keto function with amine. Finally, C−N bond formation undergoes via SN2 nucleophilic substitu-tion mode to complete aza five-membered ring, the aromatization of which yields desired product 1,2,3-trisubstituted pyrrole via conjugate transfer. Comparatively, the double bond shift in step 4 is deter-mined to be rate-limiting.

Keywords: addition-cyclization; regioselective; Tf−DMAP; pyrrole; sulfonium salt

1.Introduction

As privileged structural motifs, functionalized heterocycles are frequently encountered in pharmaceutical industry as biologically active molecules [1-3]. In this field, pyrrole is a crucial class of five-membered, nitro-gen-containing heterocycle well-known as Lipitor and dietary supplements [4,5]. In agrochemicals, flavors, and optoelectronic materials, pyrrole derivatives function as versatile building blocks. Czichy discovered elec-trochemical polymerization of pyrrole−perimidine hybrids: low-band-gap materials with high n-doping activity [6]. Zhao gave [3,4-c]pyrrole-4,6-dione-mediated crystallinity in large-band gap polymer donors directs charge transportation and recombination in efficient nonfullerene polymer solar cells [7]. Wang reported a DFT study on electroreduction NO to NH3 over single metal atom anchored on pyrrole type defective graph-eme [8]. The scaffold bearing aryl at 1-, 2-, 3-positions are particularly valuable just as Yousuf's addi-tion−annulation of arylboronic acid and substituted aliphatic nitriles in one-pot synthesis of 3-substituted 2-arylpyrrole [9]. However, the regioselective synthesis of substituted pyrroles is still challenging despite Knorr, Paal−Knorr, and Hantzsc methods [10]. Hence, facile approach to polysubstituted pyrroles is useful in organic chemistry. The crotonate-derived sulfur ylide is well-known to access carbo- and heterocyclic framework in cascade annulation. Chen researched formal [4 + 1] annulation in synthesis of carbocyclic and heterocyclic system [11]. Lu summarized recent advances in catalytic cyclization of sulfur ylides beyond sulfide-centric catalysis [12]. Gouthami achieved syntheses of 2-aroyl benzofurans through cascade annulation on arynes [13]. In addition, Kaiser found bond-forming and breaking reactions at sulfur(IV): sulfoxides, sulfonium salts, sulfur ylides, and sulfinate salts [14]. Aher gave Cp*Co(III)-catalyzed C amination/annulation cascade of sulfoxonium ylides with anthranils for the synthesis of indoloindolones [15]. Ushakov reviewed application of ylide-like species in [4 + 1]-annulation reaction [16]. Chen obtained substrate-directed divergent annulations of sulfur ylides in synthesis of functionalized bispirocyclopentane and bispirocyclopropane [17]. Thereby these building blocks combining α, β-unsaturated ester were proved to be versatile and exhibit dual reactivity [18-20]. Many progresses have been reported in this field such as rapid and scalable synthesis of oxazoles directly from carboxylic acids of Chavan group [21], triflylpyridinium enables controlled reduction of carboxylic acids to aldehydes using pinacolborane of Chen as well as coupling reagent in rapid amide and ester synthesis [22,23]. There's also novel photoswitchable molecules derived from rimonabant to highly selective and na-nomolar "cis-on" CB1R antagonist [24]. The latest breakthrough was addition–cyclization of carboxylic acid, crotonate-derived sulfonium and amine [25]. Although 1,2,3-trisubstituted pyrrole was synthesized in regi-oselective mode, how acylpyridinium salt was afforded via activation of carboxylic acid? How allyl sulfonium was deprotonated assisted by DMAP to form ylide as C3 synthon? What's the concrete process including subsequent nucleophilic attack, double bond shift, condensation, and C−N bond formation?

2. Computational details

Structures were optimized at M06-2X/6-31G(d) level with GAUSSIAN09 [26]. Among various DFT methods [27], M06-2X functional has smaller deviation between experimental and calculated value than B3LYP hybrid functional [28,29]. With 6-31G(d) basis set, it can provide best compromise between time consumption and energy accuracy. It was also found to give accurate results for stepwise (2 + 2) cycloaddition, enantioselective (4 + 3) and Diels–Alder reaction [30,31]. Together with good performance on noncovalent interaction, it is suitable for this system [32-34]. To obtain zero-point vibrational energy (ZPVE), harmonic frequency calculations were carried out at M06-2X/6-31G(d) level gaining thermodynamic corrections at 298 K and 1 atm in Toluene. At M06-2X/6-311++G(d,p) level, the solvation-corrected free energies were obtained using integral equation formalism polarizable continuum model (IEFPCM) [35-39] on M06-2X/6-31G(d)-optimized geometries. NBO procedure was performed with Natural bond orbital (NBO3.1) obtaining lone pair and bond to characterize bonding orbital interaction and electronic properties [40-42]. Using Multiwfn_3.7_dev package [43].

3. Results and Discussion

The mechanism was explored for Tf–DMAP/DMAP-catalyzed addition–cyclization of carboxylic acid 1, cro-tonate sulfonium salt 2, and amine 3 leading to 1,2,3-trisubstituted pyrrole 4 (Scheme 1). As illustrated by Scheme 2, first, the allyl sulfonium salt 2 was deprotonated assisted by DMAP to form its ylide A. Concurrently, acylpyridinium salt B was afforded upon activation of carboxylic acid 1 by TfDMAP. Subsequently, the nucleo-philic attack of A to B generates corresponding intermediate C after removal of DMAP. C converts to interme-diate D via subsequent double bond shift followed by condensation of keto function with amine 3 furnishing intermediate E. Finally, E undergoes C–N bond formation giving five-membered F, the aromatization of which yields desired 1,2,3-trisubstituted pyrrole 4. Figure 1 listed schematic structures of optimized TSs in Scheme 2. Table 1 gave activation energy for all steps.

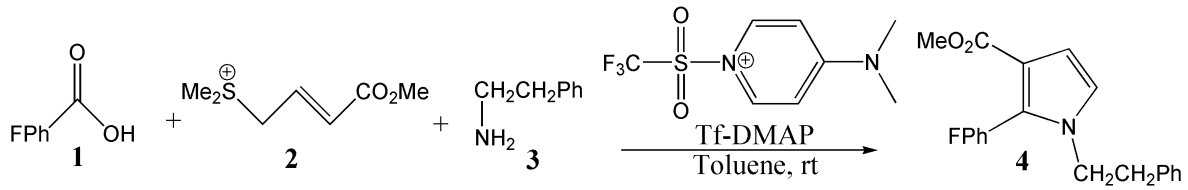

Scheme 1: Tf–DMAP/DMAP-catalyzed addition–cyclization of carboxylic acid **1**, crotonate sulfonium salt **2**, and amine **3** leading to 1,2,3-trisubstituted pyrrole **4**.

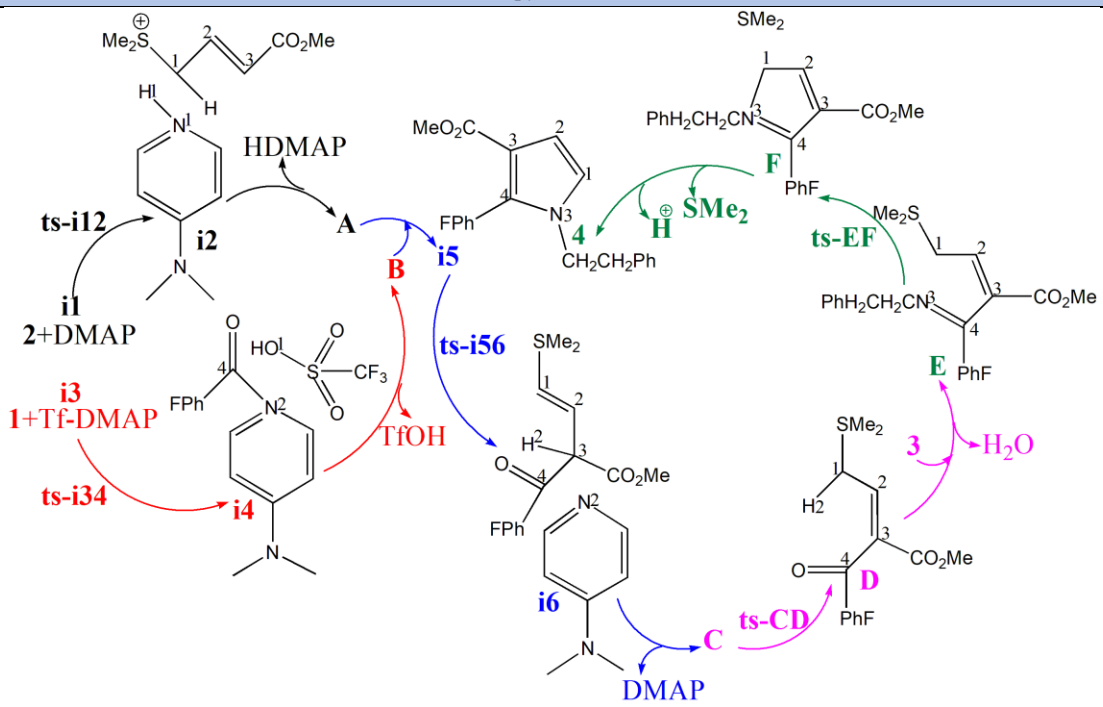

Scheme 2: Proposed reaction mechanism of Tf–DMAP/DMAP-catalyzed addition–cyclization of **1**, **2**, **3** leading to **4**. TS is named according to the two intermediates it connects.

3.1 deprotonation of allyl sulfonium/activation of carboxylic acid

Binding DMAP and allyl sulfonium salt, the first complex **i1** is formed as starting point of step 1 (black dash line of Figure 1). **2** was deprotonated under the help of DMAP via **ts-i12** with the activation energy of 16.1 kcal mol^{-1} endothermic by 11.4 kcal mol^{-1} producing reactive **i2**. The transition vector corresponds to proton transferring from C1 of **2** to N1 of DMAP as C1···H1···N1 (1.45, 1.26 Å) (Figure S1a). After proton capture by base DMAP, the ylide **A** of **2** was afforded along with its resonance-stabilized zwitterionic intermediate, of which the negative charge is located on C3 ready for nucleophilic attack.

Concurrently, the intermediate **i3** binding carboxylic acid **1** and additional TfDMAP is taken as new starting point of next step (red dash line of Figure

1). Upon activation of TfDMAP, **1** lost hydroxyl group via **ts-i34** with increased activation energy of 20.8 kcal mol^{-1} in step 2 endothermic slightly by 1.0 kcal mol^{-1} leading to **i4**. The transition vector is complicated involving breaking of C4···O1, linkage of O1···S and resultant cleavage of DMAP N2 from S to acyl C4 as S···N2···C4 (2.56, 1.8, 2.6, 2.47 Å) (Figure S1b). Once typical C4-N2 single bond is available in **i4**, the positive acylpyridinium salt **B** bonded to DMAP was generated in addition to TfOH.

TS	$\Delta G^{\neq}_{gas}$	$\Delta G^{\neq}_{sol}$
ts-i12	15.1	16.1
ts-i34	23.5	20.8
ts-i56	11.3	3.6
ts-CD	28.4	26.1
ts-EF	16.1	13.2

Table 1: The activation energy (in kcal mol^{-1}) of all reactions in gas and solvent

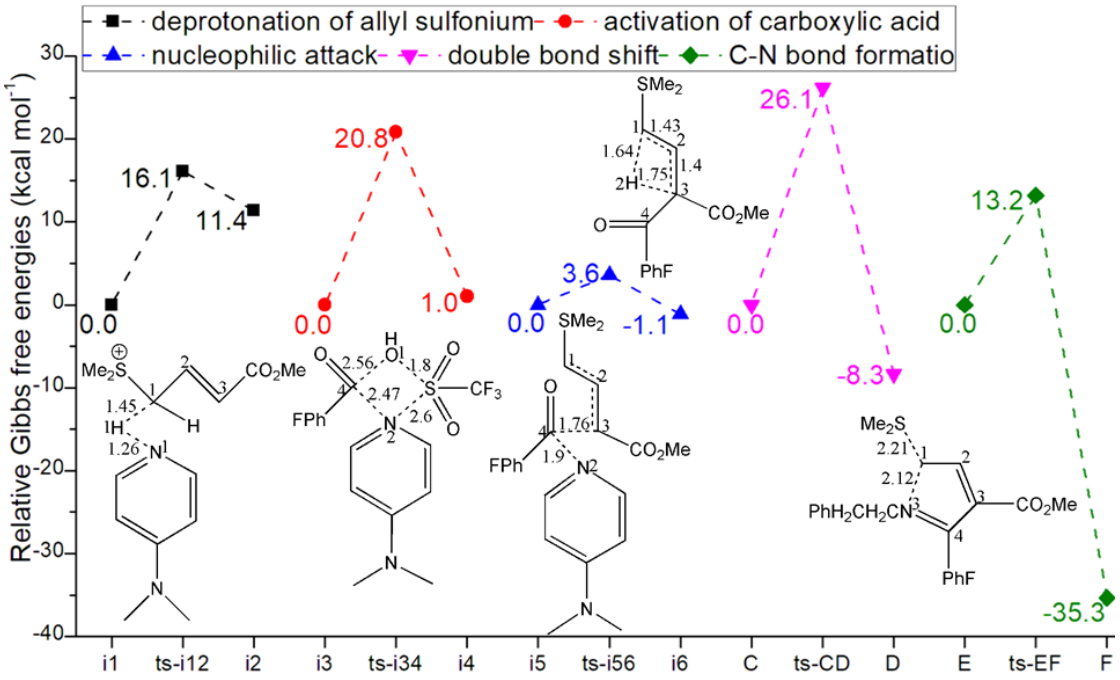

Figure 1: Relative Gibbs free energy profile in solvent phase starting from complex **i1**, **i3**, **i5**, **C**, **E** (Bond lengths of optimized TSs in Å).

3.2 nucleophilic attack/double bond shift/C−N bond formation

Subsequently, with **A** and **B** in hand, the complex **i5** was starting point of step 3 (blue dash line of Figure 1). The nucleophilic attack of **A** to **B** takes place via **ts-i56** with small activation energy of 3.6 kcal mol^{-1} exothermic by -1.1 kcal mol^{-1} giving **i6**. The transition vector of C3···C4···N2 denotes positive acyl group C4 was leaving from DMAP N2 and bonding to negative C3 (1.76, 1.9 Å). After removal of recovered DMAP, the corresponding intermediate **C** was generated with sp3 hybrid C3 and typical C1=C2 double bond.

Next, **C** converts to intermediate **D** via **ts-CD** to complete double bond shift with activation energy of 26.1 kcal mol^{-1} exothermic by -8.3 kcal mol^{-1} in step 4 (magenta dash line of Figure 1). According to the transition vector, this was achieved through proton H2 transfer from C3 to C1 as C3···H2···C1 along with shortening of C2···C3 and elongation of C1···C2 (1.75, 1.64, 1.43, 1.4 Å) (Figure S1c). The resulting **D** is stable owing to its conjugated structure involving carbonyl C4=O and new C2=C3 double bond.

With amine **3**, the condensation of keto function of **D** furnishes intermediate **E**, in which the carbonyl C4=O turns to be C4=N3 imine group. Finally, **E** undergoes C−N bond formation via **ts-EF** with decreased activation energy of 13.2 kcal mol^{-1} exothermic huge by -35.3 kcal mol^{-1} in step 5 (olive dash line of Figure 1). The transition vector suggests typical S_N2 nucleophilic substitution mode including approaching of N3 to C1 and concerted breaking down of C1-S via N3···C1···S (2.12, 2.21 Å) (Figure S1d). The C1-N3 single bond indicates aza five-membered ring is completed in last intermediate **F**. After leaving of SMe2 and one proton, C1 becomes sp2 achieving aromatization and yielding 1,2,3-trisubstituted pyrrole **4** with conjugated C1=C2, C3=C4 double bond. Comparatively, the double bond shift in step 4 is determined to be rate-limiting for Tf−DMAP/DMAP-catalyzed addition−cyclization of carboxylic acid, crotonate sulfonium and amine.

4. Conclusions

In summary, the first theoretical investigation was provided by our DFT calculation on Tf−DMAP/DMAP-catalyzed addition−cyclization of carboxylic acid, crotonate sulfonium and amine. First, the deprotonation of allyl sulfonium salt forms its ylide assisted by DMAP. Concurrently, acylpyridinium salt was afforded upon activation of carboxylic acid under the help of TfDMAP giving TfOH. Subsequently, the nucleophilic attack between the above two generates corresponding intermediate, which proceeds double bond shift followed by condensation of keto function with amine. Finally, C−N bond formation undergoes via SN2 nucleophilic substitution mode to complete aza five-membered ring, the aromatization of which yields desired 1,2,3-trisubstituted pyrrole product via conjugate transfer. Comparatively, the double bond shift in step 4 is determined to be rate-limiting for Tf−DMAP/DMAP-catalyzed addition−cyclization of carboxylic acid, crotonate sulfonium and amine.

Electronic Supplementary Material

Supplementary data available: [Computation information and cartesian coordinates of stationary points; Cal-culated relative energies for the ZPE-corrected Gibbs free energies (ΔGgas), and Gibbs free energies (ΔGsol) for all species in solution phase at 298 K.]

Author contributions: Conceptualization, Nan Lu; Methodology, Nan Lu; Software, Nan Lu; Validation, Nan Lu; Formal Analysis, Nan Lu; Investigation, Nan Lu; Resources, Nan Lu; Data Curation, Nan Lu; Writ-ing-Original Draft Preparation, Nan Lu; Writing-Review & Editing, Nan Lu; Visualization, Nan Lu; Supervision, Nan Lu; Project Administration, Nan Lu. All authors have read and agreed to the published version of the manuscript.

Funding: This work was supported by Key Laboratory of Agricultural Film Application of Ministry of Agricul-ture and Rural Affairs, P.R. China.

Conflict of interest: The authors declare no conflict of interest.

References

1. Majumdar, P.; Pati, A.; Patra, M.; Behera, R. K.; Behera, A. K. (2014). Acid Hydrazides, Potent Reagents for Syn-thesis of Oxygen-, Nitrogen-, and/or Sulfur-Containing Heterocyclic Rings. *Chem. Rev*. 114, 2942−2977.
2. Medran, N. S.; La-Venia, A.; Testero, S. A. (2019). Recent Advances in the Synthesis of C-Aryl Glycosides. *RSC Adv.* 9, 6804−6844.
3. Saha, A.; Casali, E.; Ghosh, A.; Maiti, D. (2025). Modular Approach for Photoinduced Cycloaddition Enabling the Synthesis of Diverse Bioactive Oxazoles. Org. Lett. 27 (11), 2811−2814.
4. Baidya, M.; Maiti, D.; Roy, L.; De Sarkar, S. D. (2022). Trifluoroethanol as a unique additive for the chemoselective electrooxidation of enamines to access unsymmetrically substituted NH-pyrroles. Angew. *Chem*.134 (5), No. e202111679.
5. Lade, D. M.; Pawar, A. B.; Mainkar, P. S.; Chandrasekhar, S. (2017). Total Synthesis of Lamellarin D Trimethyl Ether, Lamellarin D, and Lamellarin H. *J. Org. Chem.* 82, 4998−5004.
6. Czichy, M.; Zhylitskaya, H.; Zassowski, P.; Navakouski, M.; Chulkin, P. et al. (2020). Electrochemical Polymerization of Pyrrole−Perimidine Hybrids: Low-Band-Gap Materials with High n-Doping Activity. *J. Phys. Chem. C.* 124, 14350−14362.
7. Zhao, J.; Li, Q.; Liu, S.; Cao, Z.; Jiao, X. et al. (2020). [3,4-c]Pyrrole-4,6-Dione-Mediated Crystal-linity in Large-Bandgap Polymer Donors Directs Charge Transportation and Recombination in Efficient Nonfullerene Polymer Solar Cells. *ACS Energy Lett*. 5 (5), 367−375.
8. Wang, J.; Li, K.; Hao, Q.; Liu, D.; Zhang, X. (2023). Electroreduction NO to NH3 over Single Metal Atom Anchored on Pyrrole Type Defective Graphene: A DFT Study. *Chin. Chem.* Lett. 34, 107567.
9. Yousuf, M.; Adhikari, S. (2017). One-Pot Synthesis of 3-Substituted 2-Arylpyrrole in Aqueous Media via Addi-tion−Annulation of Arylboronic Acid and Substituted Aliphatic Nitriles. Org. Lett. 19 (9), 2214−2217.
10. Reddy, N. N. K.; Rawat, D.; Adimurthy, S. (2018). Visible-Light-Induced C (sp3)−H Functionalization of Tosylhy-drazones: Synthesis of Polysubstituted Pyrroles under Metal-Free Conditions. *J. Org. Chem.* 83, 9412−9421.
11. Chen, J.-R.; Hu, X.-Q.; Lu, L.-Q.; Xiao, W.-J. (2015). Formal [4 + 1] Annulation Reactions in the Synthesis of Car-bocyclic and Heterocyclic Systems. *Chem. Rev.*115 (11), 5301−5365.
12. Lu, L. Q.; Li, T. R.; Wang, Q.; Xiao, W. J. (2017). Beyond Sulfide-centric Catalysis: Recent Advances in the Catalytic Cyclization Reactions of Sulfur Ylides. *Chem. Soc.* Rev. 46, 4135−4149.
13. Gouthami, P.; Chavan, L. N.; Chegondi, R.; Chandrasekhar, S. (2018). Syntheses of 2-Aroyl Benzofurans Through Cascade Annulation on Arynes. *J. Org. Chem*. 83 (6), 3325−3332.
14. Kaiser, D.; Klose, I.; Oost, R.; Neuhaus, J.; Maulide, N. (2019). Bond-Forming and Breaking Reactions at Sul-fur(IV): Sulfoxides, Sulfonium Salts, Sulfur ylides, and Sulfinate Salts. *Chem. Rev*. 119, 8701−8780.
15. Aher, Y. N.; Pawar, A. B. (2021). Cp*Co(III)-Catalyzed C Amination/Annulation Cascade of Sulfoxonium Ylides with Anthranils for the Synthesis of Indoloindolones. *Chem. Commun*. 57, 7164−7167.
16. Ushakov, P. Y.; Ioffe, S. L.; Sukhorukov, A. Y. (2022). Recent Advances in the Application of Ylide-Like Species in [4 + 1]-Annulation Reactions: An Update Review. *Org. Chem. Front,* 5358−5382.
17. Chen, S.; Liang, P.; Cai, Y.; Zhou, L.; Wang, S. (2024). Substrate-directed divergent annulations of sulfur ylides: synthesis of functionalized bispirocyclopentane and bispirocyclopropane derivatives. *Org. Biomol. Chem*. 22 (11), 2197−2202.
18. Jia, P.; Huang, Y. (2016). Sequential Annulation Domino Reaction of Sulfur Ylides and α,β-Unsaturated Cyclic Ketimines: Synthesis of Cyclic 2-Alkenyl Aziridines. *Org. Lett*, 18, 2475−2478.
19. Li, J.-L.; Dai, Q.-S.; Yang, K.-C.; Liu, Y.; Zhang, X. (2018). Construction of Azepino[2,3-b]indole Core via Sulfur Ylide Mediated Annulations. *Org. Lett*, 20, 7628−7632.
20. Xiong, D.; Wang, L.; Qu, X.; Chen, Y.; Li, L. et al. (2026). Recent Advances in Diverse Reac-tions of γ-Bromocrotonates and Their Derived Allyl Sulfonium Salts. *Chem. Commun*.62, 1045−1057.
21. Chavan, L. N.; Pashikanti, G.; Goodman, M. M.; Liebeskind, L. S. (2025). Rapid and Scalable Synthesis of Oxazoles Directly from Carboxylic acids. *J. Org. Chem*. 90 (10), 3727−3732.

22. Chen, D.; Xu, L.; Yu, Y.; Mo, Q.; Qi, X. et al. (2023). Triflylpyridinium Enables Rapid and Scalable Controlled Reduction of Carboxylic Acids to Aldehydes using Pinacolborane. *Angew. Chem*. 135, No. e202215168.
23. Chen, D.; Xu, L.; Ren, B.; Wang, Z.; Liu, C. (2023). Triflylpyridinium as Coupling Reagent for Rapid Amide and Ester Synthesis. *Org. Lett.* 25, 4571−4575.
24. Rodríguez-Soacha, D. A.; Fender, J.; Ramírez, Y. A.; Collado, J. A.; Munoz, E. (2021). "Photo-Rimonabant": Synthesis and Biological Evaluation of Novel Photoswitchable Molecules Derived from Rimonabant Lead to a Highly Selective and Nanomolar "Cis-On" CB1R Antago-nist. ACS Chem. *Neurosci*.12, 1632−1647.
25. Chavan, L. N.; Pashikanti, G.; Goodman, M. M.; Liebeskind, L. S. (2026). Regioselective Synthesis of 1,2,3-Trisubstituted Pyrroles via Addition–Cyclization of Crotonate-Derived Sulfonium Salts with a Car-boxylic Acid and an Amine. *J. Org. Chem.* 2026, 91, 10, 3776–3788.
26. Frisch, M. J.; Trucks, G. W.; Schlegel, H. B. et al. (2010). Gaussian 09 (Revision B.01), Gaussian, Inc., Wallingford, CT.
27. Stephens, P. J.; Devlin, F. J.; Chabalowski, C. F.; Frisch, M. J. (1994). Ab initio Calculation of Vibrational Absorp-tion and Circular Dichroism Spectra Using Density Functional Force Fields, *J. Phys. Chem*. 98, 11623-11627.
28. Becke, A. D. (1996). Density-functional thermochemistry. IV. A new dynamical correlation functional and implica-tions for exact-exchange mixing. *J. Chem. Phys*. 104, 1040-1046.
29. Lee, C. T.; Yang,W. T.; Parr, R. G. (1988). Development of the Colle-Salvetti correlation-energy formula into a functional of the electron density. Phys. Rev. B. 37, 785-789.
30. Li, X.; Kong, X.; Yang, S.; Meng, M.; Zhan, X. et al. (2019). Bifunctional Thiourea-Catalyzed Asym-metric Inverse-Electron-Demand Diels-Alder Reaction of Allyl Ketones and Vinyl 1,2-Diketones via Dieno-late Intermediate, *Org. Lett*. 21, 1979-1983.
31. Krenske, E. H.; Houk, K. N.; Harmata, M. (2015). Computational Analysis of the Stereochemical Outcome in the Imidazolidinone-Catalyzed Enantioselective (4 + 3)-Cycloaddition Reaction, *J. Org. Chem*. 80, 744-750.
32. Lv, H.; Han, F.; Wang, N.; Lu, N.; Song, Z. (2022). Ionic Liquid Catalyzed C-C Bond Formation for the Synthesis of Polysubstituted Olefins. *Eur. J. Org. Chem*. e202201222.
33. Zhuang, H.; Lu, N.; Ji, N.; Han, F.; Miao, C. (2021). Bu4NHSO4-Catalyzed Direct N-Allylation of Pyrazole and its Derivatives with Allylic Alcohols in Water: A Metal-free, Recyclable and Sustainable System. *Advanced Synthesis & Catalysis*, 363, 5461-5472.
34. Lu, N.; Liang, H.; Qian, P.; Lan, X.; Miao, C. (2020). Theoretical investigation on the mechanism and enantioselec-tivity of organocatalytic asymmetric Povarov reactions of anilines and aldehydes. *Int. J. Quantum Chem*, 120, e26574.
35. Tapia, O. (1992). Solvent effect theories: Quantum and classical formalisms and their applications in chemistry and biochemistry. *J. Math. Chem*. 10, 139-181.
36. Tomasi, J.; Persico, M. (1994). Molecular Interactions in Solution: An Overview of Methods Based on Continu-ous Distributions of the Solvent. *Chem. Rev*. 94, 2027-2094.
37. Simkin, B. Y.; Sheikhet, I. (1995). Quantum Chemical and Statistical Theory of Solutions—A Computational Ap-proach, Ellis Horwood, London.
38. Tomasi, J.; Mennucci, B.; Cammi, R. (2005). Quantum Mechanical Continuum Solvation Models. *Chem. Rev*, 105, 2999-3093.
39. Marenich, A. V.; Cramer, C. J.; Truhlar, D. G. (2009). Universal Solvation Model Based on Solute Electron Density and on a Continuum Model of the Solvent Defined by the Bulk Dielectric Constant and Atomic Surface Tensions. *J. Phys. Chem*. B, 113, 6378–6396.
40. Reed, A. E.; Weinstock, R. B.; Weinhold, F. (1985). Natural population analysis. *J. Chem. Phys*. 83, 735-746.
41. Reed, A. E.; Curtiss, L. A.; Weinhold, F. (1988). Intermolecular interactions from a natural bond orbital do-nor-acceptor view point. *Chem. Rev.* 88, 899-926.
42. Foresman, J. B.; Frisch, A. (1996). Exploring Chemistry with Electronic Structure Methods, 2nd ed., Gaussian, Inc., Pittsburgh.
43. Lu, T.; Chen, F. (2012). Multiwfn: A multifunctional wavefunction analyzer. *J. Comput. Chem*. 33, 580-592.

DOI:10.31579/2693-4779/329